Pacific Northwest
NATIONAL LABORATORY

PNNL-38692

Development of Low-cost Magnetocaloric Materials (CRADA 446)

November 2025

Mert Efe
Robin Ihnfeldt
Aashish Rohatgi

U.S. DEPARTMENT OF ENERGY

Prepared for the U.S. Department of Energy
under Contract DE-AC05-76RL01830

DISCLAIMER

PACIFIC NORTHWEST NATIONAL LABORATORY
operated by
BATTELLE
for the
UNITED STATES DEPARTMENT OF ENERGY
under Contract DE-AC05-76RL01830

Printed in the United States of America

Available to DOE and DOE contractors from
the Office of Scientific and Technical Information,
P.O. Box 62, Oak Ridge, TN 37831-0062
www.osti.gov
ph: (865) 576-8401
fox: (865) 576-5728
email: reports@osti.gov

Available to the public from the National Technical Information Service
5301 Shawnee Rd., Alexandria, VA 22312
ph: (800) 553-NTIS (6847)
or (703) 605-6000
email: info@ntis.gov
Online ordering: http://www.ntis.gov

PNNL-38692

Development of Low-cost Magnetocaloric Materials (CRADA 446)

November 2025

Mert Efe
Robin Ihnfeldt
Aashish Rohatgi

Prepared for
the U.S. Department of Energy
under Contract DE-AC05-76RL01830

Pacific Northwest National Laboratory
Richland, Washington 99354

Cooperative Research and Development Agreement (CRADA) Final Report

Report Date: 18th November 2025

In accordance with Requirements set forth in the terms of the CRADA, this document is the CRADA Final Report, including a list of Subject Inventions, to be provided to PNNL Information Release who will forward to the DOE Office of Scientific and Technical Information as part of the commitment to the public to demonstrate results of federally funded research.

Parties to the Agreement: General Engineering & Research, LLC (GE&R) and Pacific Northwest National Laboratory

CRADA number: 446

CRADA Title: Development of Low-cost Magnetocaloric Materials

Responsible Technical Contact at DOE Lab: Aashish Rohatgi

Name and Email Address of POC at Company: Robin Ihnfeldt, rihnfeldt@geandr.com

DOE Program Office: Hydrogen and Fuel Cell Technology Office

Joint Work Statement Funding Table showing DOE funding commitment:

Funding	Project Year 1	Project Year 2	TOTALS
Government			
DOE	$150,000	$200,000	$350,000
Other			
Total Govt.	**$150,000**	**$200,000**	**$350,000**
Participant			
In-Kind	$150,000	$200,000	$350,000
Funds-In			
FAC			
Total Participant	**$150,000**	**$200,000**	**$350,000**
TOTAL CRADA Value	**$300,000**	**$400,000**	**$700,000**

Acknowledgments

The authors gratefully acknowledge support from Neha Rustagi, technology manager at the Hydrogen & Fuel Cell Technology Office, U.S. Department of Energy. The authors would like to acknowledge the following PNNL staff: Anthony Guzman for sample preparation, Xiaolong Ma, Nathan Canfield, and Jarrod Crum for SEM/EDS, Jose Marcial for XRD analysis, and John Barclay for technical discussions.

Executive Summary

The overall goal of this project was to develop an energy-efficient technique to shorten the annealing time of magnetocaloric materials (MCM), from days to hours, with the expected benefits of lower costs and shorter lead times. Success in this project will enable industry partner General Engineering & Research LLC (GE&R) to commercialize their high-performance MCM, in support of DOE-Hydrogen & Fuel Cell Technology Office's efforts to develop energy-efficient magnetic refrigeration technology (using MCM) for hydrogen liquefaction.

Towards this goal, GE&R acquired and installed a new vacuum arc-melter which allowed them to cast the CeSi in new shapes and with better chemical homogeneity. PNNL integrated their existing Joule-heating system within a vacuum chamber that allowed oxidation-sensitive CeSi alloy to be annealed in a controlled atmosphere with reduced oxidation. Additional annealing experiments were performed using a conventional furnace. The samples' magnetocaloric performance and microstructure were characterized using optical and electron microscopy techniques and x-ray diffraction. Simple diffusion-based equations were used to explain the results.

Both heating methods showed similar results and the annealing duration could be shortened from 18 days to just 7 hours, resulting in estimated 99% lower energy consumption and 87% lower process costs. Since as-cast Ce-Si binary system can form a variety of phases, small changes in phase fractions were found to influence magnetocaloric performance greatly. The relatively fast diffusion of Ce atoms during annealing is hypothesized to contribute to "short" annealing durations that help transform undesirable phases into desirable phases within 7 hours with improved magnetocaloric performance. The results point to precise chemistry of the starting materials and appropriate heat-treatments to produce desirable phases, to produce MCMs with the best performance.

Table of Contents

Introduction

Magnetocaloric materials (MCM) refer to a set of materials that undergo temperature changes when exposed to a varying magnetic field. This phenomenon is harnessed in magnetic refrigeration technologies that are more energy efficient than the conventional vapor-compression based cooling technologies for liquefaction of gases such as H2.

Rare-earth intermetallics, particularly silicides, are good candidate MCMs as they have strong magnetocaloric properties originating from first and/or second order phase transformations. While the magnetocaloric effect from the first order transformations is much larger than that from the second order transformation, it occurs only over a narrow temperature range and is usually accompanied by a large volume change and hysteresis [1]. Materials with second order phase transformations (SOPT) are more suitable for magnetic refrigeration in the cryogenic range. However, their smaller entropy (ΔS_m) and adiabatic temperature change (ΔT_{ad}) need to be maximized by carefully controlling the composition and microstructure of the material. Examples of rare-earth based MCM with SOPT are: relatively expensive rare-earth (Gd, Tb, Dy, Er) based Laves phases ($MgCu_2$ type structure), some members of the $Gd_5(Si,Ge)_4$ family of alloys, and Fe_3C structured alloys [1].

The higher cost of some of the rare-earth elements such as Gd, Tb, Dy, and Er has pushed researchers to develop alternative alloys with relatively inexpensive rare-earths. Accordingly, as a much affordable alternative, rare-earth silicides have recently been discovered and commercialized by General Engineering & Research LLC (GE&R) [2-4] and are commercially available for purchase directly [5]. GE&R alloys are Ge free and contain low-cost cerium and gadolinium based (cerium is ~ 10x cheaper than Nd, Er, Ho and ~ 100x cheaper than Dy, Tb). These silicides can be classified as a sub-category of $Gd_5(Si,Ge)_4$ family of intermetallics and their composition can be tuned to show magnetocaloric effect over a wide temperature range (Figure 1). Among these compositions, cerium silicides demonstrate large magnetic entropy change from SOPT around 4-10 K, making them ideal candidates for hydrogen liquefication through magnetic refrigeration [6, 7].

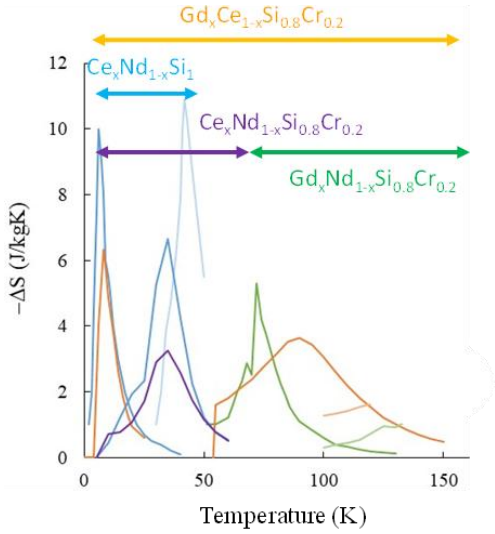

Figure 1. Magnetocaloric performance of Ce, Nd, Gd containing alloys over a wide temperature range. Ce-based alloys operate at temperatures relevant to hydrogen liquefication and demonstrate significantly high magnetocaloric effect. Data from GE&R.

Compounds of the $Gd_5(Si,Ge)_4$ family can have quite different crystal structures based on the stoichiometry and at the far-end of only Ge or Si-based compounds, Gd_5Si_4 or Gd_5Ge_4, have orthorhombic structure (Pnma space group) [1, 8]. Even for a single stoichiometry, it is hard to produce these alloys with desired microstructure and properties. Polymorphism, existence of detrimental phases, and inhomogeneities in the as-cast state are some of the reasons that decrease the magnetocaloric performance of these alloys [1, 9-11]. One common example to detrimental phase is the precipitation of the hexagonal, antiferromagnetic Gd_5Si_3 during casting, which is detrimental for the magnetocaloric behavior [12]. Precipitation of undesired, antimagnetic phases has also been a common problem in other types of MCM [13-16]. GdScSi ternary alloy shows remnants of detrimental phases even after annealing at 800 °C for one month [17]. Therefore, as-cast pieces of these alloys are annealed at high temperatures (> 1000 °C) for days to weeks to homogenize the microstructure and achieve the desired properties. The $(Ce, Nd, Gd)_xSi_{1-x}$ system is unfortunately no different from its predecessors and requires 10-20 days of annealing at 1100 – 1500 °C to maximize its magnetocaloric properties [6, 8, 18]. GE&R fabricates the MCM by casting ingots that need to be annealed in vacuum/inert gas furnaces at ~950-1500 °C for up to six weeks to produce a homogeneous MCM. Such extremely long heat-treatments add to the overall cost and increase the lead time to market.

There are few studies available on $Ce_5(Si,Ge)_4$ system, and binaries of Ce-Si and Nd-Si [19-22]. Magnetic and magnetocaloric properties have only been reported for the $Ce_5(Si,Ge)_4$ system [19]. Depending on the stoichiometry, the binary alloys (i.e. Ce-Si and Nd-Si) can have a range of crystal structures, with orthorhombic phase (FeB type) for the 1:1 CeSi or NdSi compounds. Some of the phases may be detrimental to the magnetocaloric performance and appear as precipitates, as in the case of $Gd_5(Si,Ge)_4$ system. Indeed, $CeSi_{2-a1}$ type precipitates (orthorhombic α-$GdSi_2$ type) have been observed in CeSi alloys [20]. A slight change in the silicon content of Si-rich silicides can have a large effect on the magnetic properties [23]. However, lack of any detailed microstructural characterization studies on the Ce-Si system prevents a complete understating of the phases present, phase transformation behavior and their effect on the magnetic properties. Therefore, a systematic study is needed on the effects of annealing process parameters on the microstructure development in the Ce-Si alloys. Such knowledge would allow us to understand the formation of detrimental phases, eventually leading to the ability to control/prevent their formation through processing and simplifying (or eliminating altogether) annealing treatments.

Objectives

Based on the technical challenges experienced by GE&R and the findings from the literature, this project had two sets of objectives on 1) reducing the annealing times and 2) microstructural characterization to understand the phase evolution during casting and annealing. The first part of the project focused on process development for the purpose of shortening annealing time. Our hypothesis was acceleration of diffusion and therefore annealing kinetics using PNNL's Joule-heating method (US patent 11,028,470). In the second part of the project, microstructural characterization was performed to understand mechanisms responsible for the improvement of magnetocaloric performance with lengthy annealing treatments. Our hypothesis was that the detrimental phases, formed during the material fabrication during casting, were responsible for the reduced performance in the as-cast materials.

The sub-objectives for the first part (processing) of the project were:

Objective 1-1: Develop Joule-heating parameters to shorten the process time for the selected MCM.

Objective 1-2: Determine cost-saving potential of Joule-heating process for MCM.

The sub-objectives for the second part (microstructural characterization) of the project were:

Objective 2-1: Understand the effects of casting and annealing processes on the microstructure development of GE&R's alloys with high resolution characterization techniques.

Objective 2-2: Understand the phase transformation and kinetics behavior of the MCM alloys by in-situ techniques.

Experimental Approach

The CeSi alloys were cast by GE&R using an Arc 200 arc melting system from Arcast, Inc, which was acquired as part of this project. The starting materials of elemental Cerium (from Ganzhou Wanfeng Adv. Materials Tech. Co., Ltd.) and Silicon (from Exotech, Inc.) were both 99.99% purity and measured using an Intell-Lab Balance with 0.0001 g accuracy. The Arc 200 uses a cold crucible process under Argon atmosphere with electromagnetic stirring capability to fully homogenize the alloy.

The as-cast samples were later annealed in a controlled-atmosphere furnace or by PNNL's Joule-heating method. Both anneals were performed under a dilute mixture of argon and hydrogen gases to prevent the oxidation of samples. For the Joule-heating method, a special vacuum-chamber was designed and fabricated with the capability of heating MCM sample to 1000 °C in vacuum/slightly reducing atmosphere, without significant oxidation (Figure 2). The setup had the samples sandwiched between graphite electrodes, which supplied pulsed currents between 200-750 A at 2-5 V for Joule heating with precise and stable temperature control. The MCM samples were found to be very brittle that necessitated additional modifications to the sample holder design to compensate for thermal expansion at the elevated temperature.

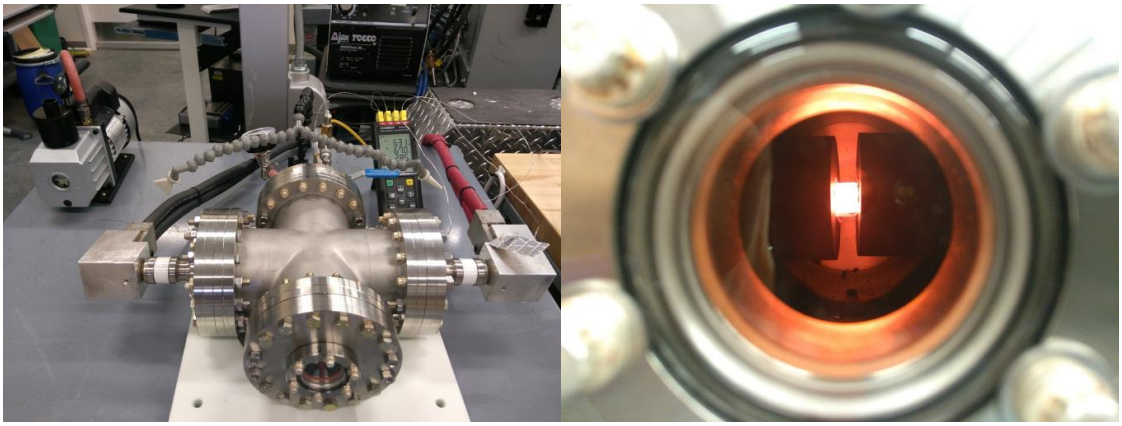

(a) (b)

Figure 2. PNNL's 2nd generation MCM Joule-heating setup. (a) Overall view; MCM samples can be annealed in vacuum or controlled atmosphere. (b) Looking into the vacuum chamber through a glass window at a red-hot MCM sample being annealed through Joule-heating while being held between two graphite electrodes.

To characterize the magnetocaloric properties, a VersaLab Physical Property Measurement System with a Vibrating Sample Magnetometer from Quantum Design, Inc. was used. This method of characterization measures the magnetization curves at various temperatures, and then the entropy change ΔS_M is calculated using the Maxwell relation:

$$\Delta S_M(T, \Delta H) = S_M(T, H) - S_M(T, 0) = \int_0^H \left(\frac{\partial M}{\partial T}\right) dH$$

As-cast and annealed samples were characterized by ex-situ and in-situ X-ray diffraction (XRD). Ex-situ XRD consisted of scanning the samples in 5-90° 2θ angles, identifying the phases, and

using Rietveld refinement to calculate the phase fractions in weight percent. In-situ XRD consisted of heating samples to 1000 °C with a hot stage under controlled atmosphere and measuring the XRD at the same 2θ angle range every half an hour. Due to high reactivity of the MCM samples, it was not possible to get reliable XRD data at high temperatures without significant oxidation of the samples. Heating under vacuum or with a zirconium getter in the existing system did not prevent oxidation.

As-cast and annealed MCM samples were polished and swabbed with 30 ml nitric and 25 ml glycerin solution for a tint etch that revealed the phases for optical microscopy. Polished samples were also imaged with scanning electron microscopy using backscattered imaging and compositions were analyzed by energy-dispersive X-ray spectroscopy.

Results & Discussion

Furnace annealing of cast CeSi samples at 1100 °C for 18 days significantly improves their magnetocaloric performance as measured by the entropy change and adiabatic temperature change (Figure 3). The magnetic entropy change is close to zero or sometimes positive around 5 K for the as-cast samples. Annealed samples show $-\Delta S_m$ of 5-11 J/kgK under 3 T magnetic field, which is slightly below the reported values in the literature (~ 14 J/kgK) for CeSi samples tested under 50 kOe magnetic field [6]. The positive entropy change observed around 5 K disappears after annealing, whereas the adiabatic temperature change for SOPT is 5-15 K. Magnetocaloric effect in the annealed CeSi is sensitive to the starting composition as discovered by GE&R. Samples containing slightly higher cerium, to compensate for the evaporation losses during arc melting, have twice the entropy change compared to the stoichiometric CeSi (Figure 3). Temperature at ΔS_{max} also depends on the composition and it shifts down to 7 K from 9 K for the off-stoichiometric $Ce_{1.02}Si$.

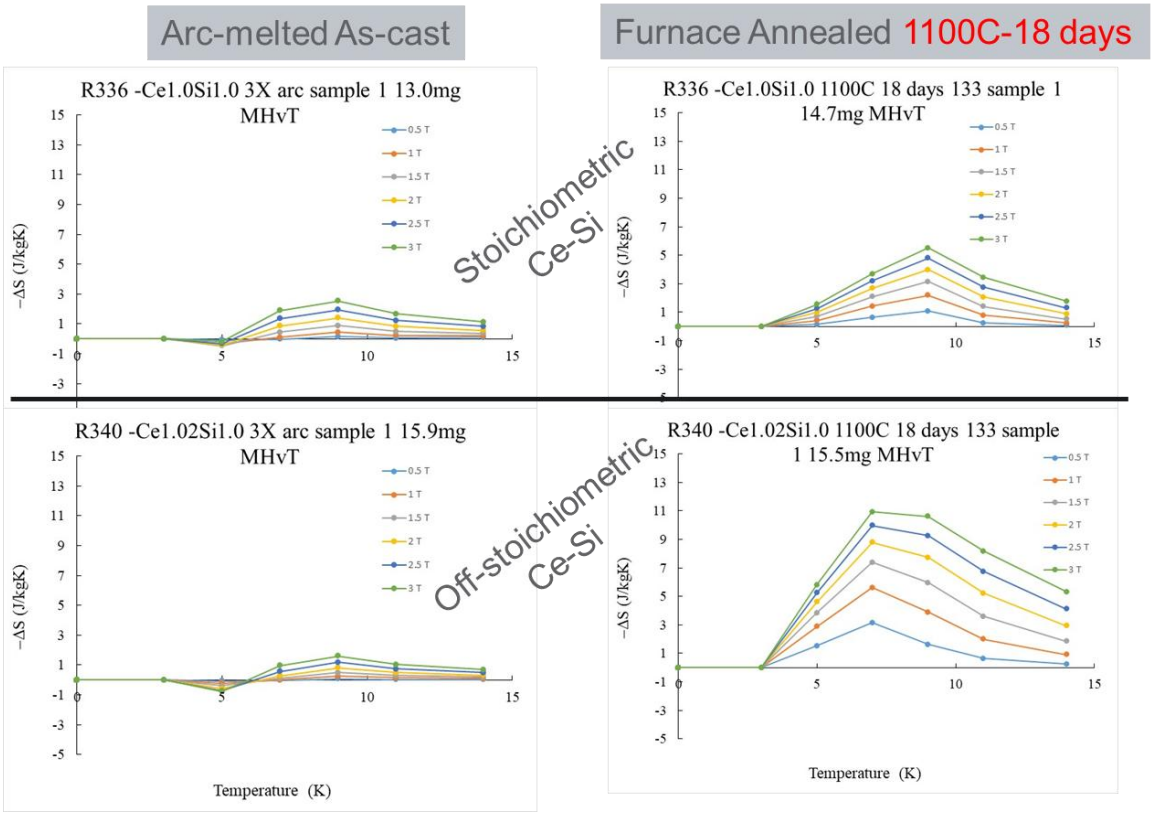

Figure 3. Magnetocaloric performance of as-cast and annealed stoichiometric CeSi and off-stoichiometric $Ce_{1.02}Si$ demonstrating that annealing and off-stoichiometric composition improve the magnetocaloric performance.

Compositional dependance of the magnetocaloric effect (MCE) i.e. off-stoichiometric $Ce_{1.02}Si$ showing almost double the MCE performance than stoichiometric Ce-Si (Figs. 3b and 3d), can be explained by the difference in phase fractions in the microstructure. XRD results show CeSi as the major matrix phase (~80-90%) with minor weight fractions of $CeSi_{1.8}$, $CeSi_2$, Ce_2Si_3, and Ce_5Si_4 both in the as-cast and annealed samples (Table 1). While the phase fraction changes are small between the as-cast and annealed and within the detection and refinement error, it is

possible to observe a significant difference in the phase fractions CeSi and $Ce_{1.02}Si$. The Ce_2Si_3 fraction (in both as-cast and annealed samples) is significantly lower and the CeSi phase fraction is slightly higher in the off-stoichiometric composition compared to the stoichiometric CeSi suggesting that Ce_2Si_3 may be detrimental for the MCE.

Table 1. Major phases present and their weight fractions in as-cast and annealed CeSi and $Ce_{1.02}Si$.

Phase fractions in wt.%	***CeSi***	***$CeSi_{1.8}$***	***$CeSi_2$***	***Ce_2Si_3***	***Ce_5Si_4***
CeSi, as-cast	87	2	2	6	2
CeSi, annealed 1100 °C 18 days	84	1	1	9	3
$Ce_{1.02}Si$, as-cast	91	-	2	1	3
$Ce_{1.02}Si$, annealed 1100 °C 18 days	90	1	2	3	3

A closer look into the samples by optical microscopy reveals the phase differences between the as-cast and annealed samples (Figure 4). As-cast microstructures are dendritic and contain a white-etched phase along the boundaries. The dendrite size is in the order of millimeters. Another microstructural feature is the thin, dark lines, which can be an additional phase. There is also some cracking and porosity present in the sample originating from the arc-melting process and the very brittle nature of the samples. Annealed samples, on the other hand, have a higher fraction of the dark phase and dark regions adjacent to the white phase. Dendrite size seems to be slightly larger than the as-cast.

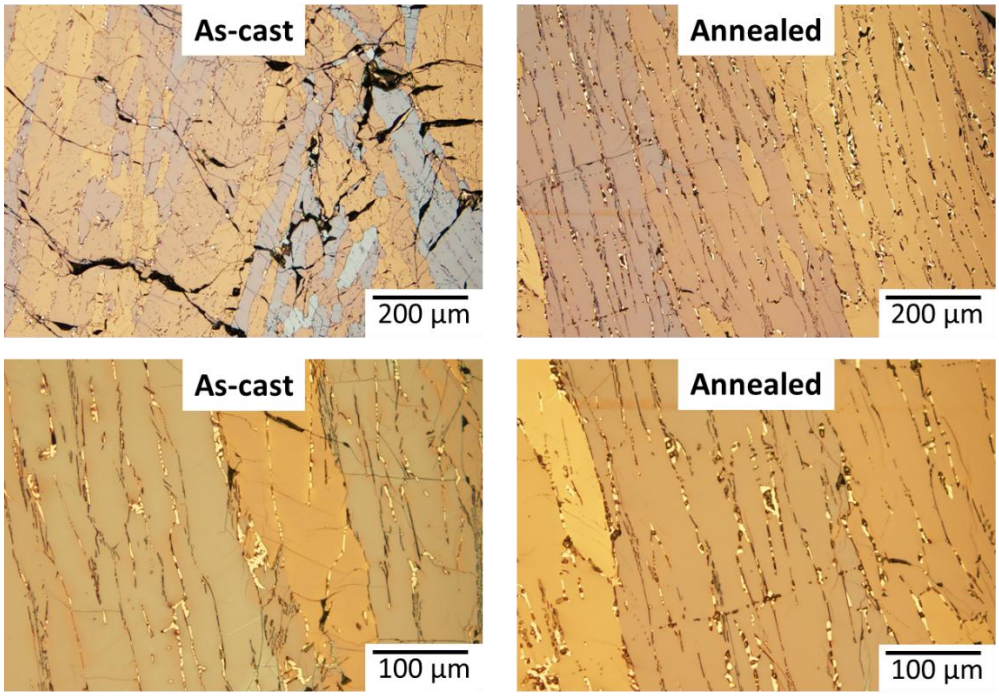

Figure 4. Optical microstructures of (left) as-cast $Ce_{1.02}Si$ and (right) 1100 °C – 18 days annealed $Ce_{1.02}Si$ showing that the annealed samples have a higher fraction of the dark phase along the grain boundaries relative to the as-cast samples.

Backscattered electron images from SEM (Figure 5) also confirm the phases observed in optical microscopy except that the contrast is reversed compared to the optical micrographs. Based on

their size and shape, white phase in optical microscopy appears as dark, black phases in SEM, whereas thin, black line phases in optical microscopy appear as light gray in SEM. The dark, round phase in optical microscopy corresponds to bright, white in the SEM of the annealed sample. These phases usually occur adjacent to their black counterparts. EDS point and area scans from multiple locations identify the black phases as Si rich with likely composition of Ce_2Si_3, light gray line phases as, and white, bright phases as Ce rich with a likely composition of Ce_5Si_4 (Figure 5). The overall composition of the matrix is slightly Ce rich (51.7 at%), likely due to the initial off-stoichiometric (Ce-rich) $Ce_{1.02}Si$ composition.

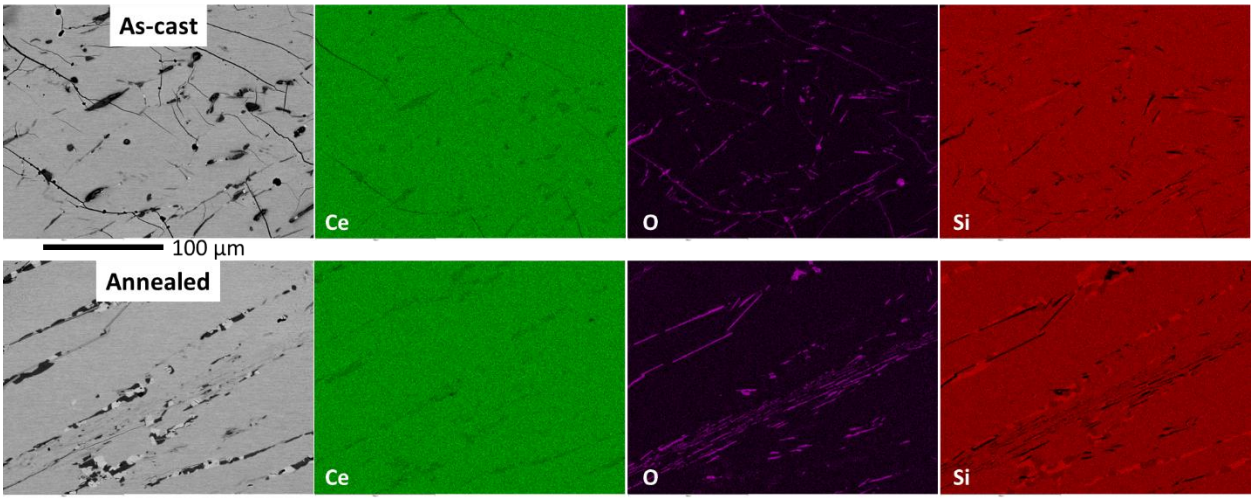

Figure 5. SEM backscattered electron images of (top) as-cast and (bottom) annealed $Ce_{1.02}Si$ and elemental distribution maps of Ce, O, and Si from the image areas. These images and maps confirm the transformation of Si-rich phases in the as-cast sample to Ce-rich phases in the annealed sample.

Line scans from the matrix phase CeSi in the as-cast and annealed samples (Figure 6) show similar variation in the Ce and Si compositions, with Ce slightly lower in the annealed (51.35 vs 51.44 at.%). Similar average Ce content of as-cast and annealed samples indicates that there was no significant segregation or inhomogeneity in the elemental distribution after the arc-melting and casting. Triple arc-melting before casting helped with homogeneity. Therefore, the increase in MCE after annealing cannot be explained by homogenization alone. Fractions of the Ce_2Si_3 and Ce_5Si_4 phases, on the other hand, show significant changes after annealing. The as-cast samples contain mostly Si-rich Ce_2Si_3 with some CeO_2. Ce_5Si_4 emerges after annealing in the form of bright, white regions. Image analysis of multiple SEM images from random locations combined with EDS allowed a first order area fraction estimate of the phases in the as-cast and annealed samples. The amount of CeO_2 appears to be higher in the annealed sample, while Ce_5Si_4 is only present in the annealed sample with 1.1% area fraction. Ce_2Si_3 phase fraction decreases from 2% in the as-cast to 1.5% in the annealed sample.

Formation of $CeSi_{2-x}$ phase with a nominal composition of Ce_2Si_3 was also observed in ball-milling and spark plasma sintering synthesis of various cerium silicides, including CeSi [24]. While XRD indicates this phase is $CeSi_{2-x,}$ EDS confirms it as Ce_2Si_3. Ce_2Si_3 forms as an intermediate phase and then reacts with excess Ce and/or Si to form the desired silicide [24]. This is in line with our observations of annealing decreasing the fraction of Ce_2Si_3 and increasing the fraction of CeSi. Alanko et al. were unable to synthesize and observe Ce_5Si_4, but Ce-rich Ce_5Si_3 was also present as an intermediate phase in the CeSi target silicide [24].

Therefore, it is expected to form intermediate Ce-rich and Si-rich silicides during initial reaction of elemental Ce and Si. In our case this reaction produced Si-rich Ce_2Si_3 and then converted it to CeSi and Ce_5Si_4, which is consistent with the literature observations.

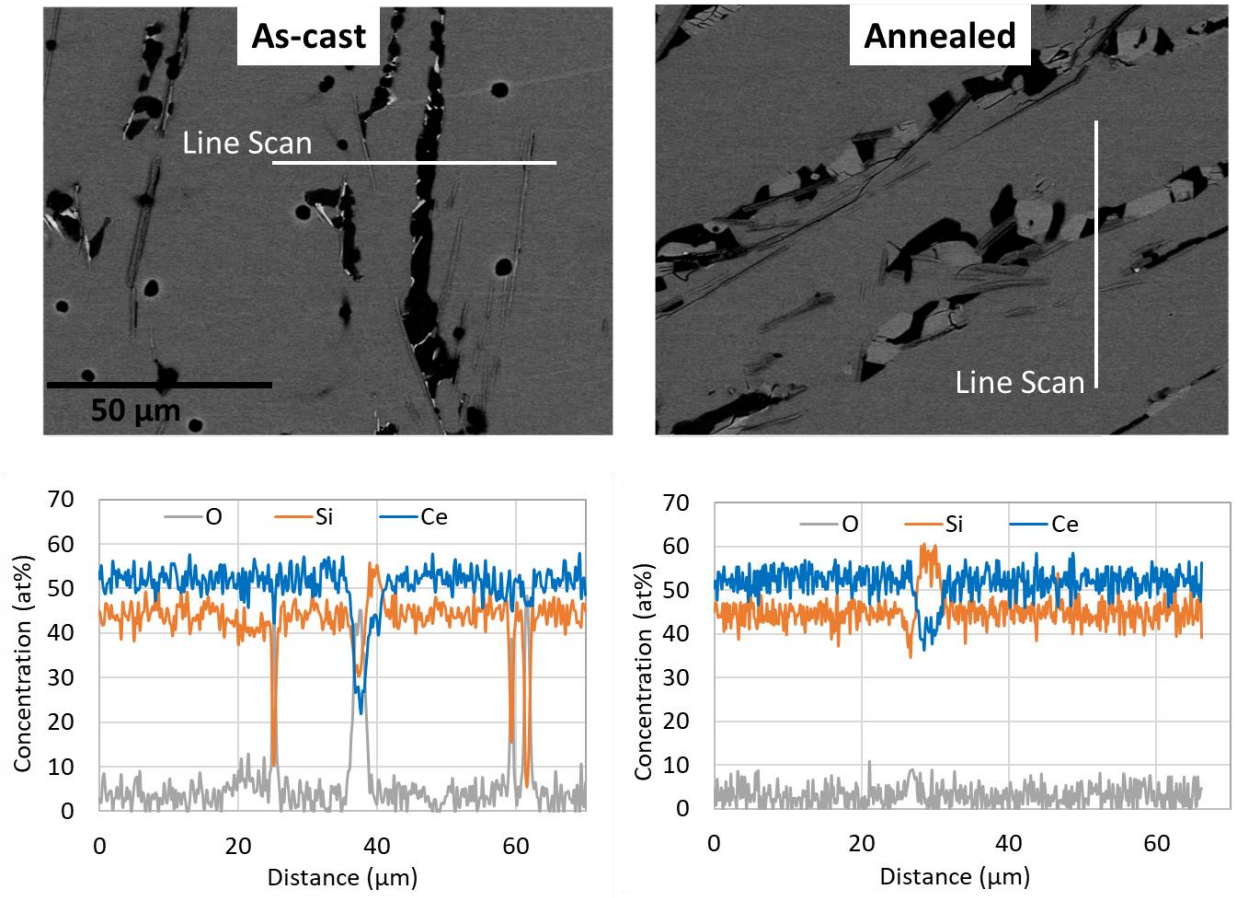

Figure 6. SEM backscattered electron images of (left) as-cast and (right) annealed $Ce_{1.02}Si$ and EDS line scans showing that the matrix concentration of Ce, O, and Si are similar in the matrices of both the materials and the Ce_2Si_3 phase is present in both as well.

Based on the literature [6, 25] both CeSi and Ce_5Si_4 phases demonstrate antiferromagnetic-paramagnetic transformations with negative and large ΔS_m around 5.6 and 6 K. The small, positive ΔS_m seen in the as-cast samples around 5 K is due to the antiferromagnetic to ferromagnetic transformation typical in CeSi phase and it disappears after annealing [6, 26]. Ce_2Si_3 phase, on the other hand, demonstrates ferromagnetic-paramagnetic transformation around 13 K [27, 28], which may work against the antiferromagnetic-paramagnetic transformations in CeSi. The improvement in MCE (larger, negative ΔS_m) with the as-cast $Ce_{1.02}Si$ samples can then be explained by the reduction of Ce_2Si_3 phase fraction shown by XRD. EDS analysis of the annealed samples also indicates the common culprit as the Ce_2Si_3 phase. Further, emergence of the Ce_5Si_4 phase after annealing should help with the MCE as its magnetocaloric effect is same with the CeSi at similar temperatures [25]. Therefore, combined XRD and EDS results and the microscopy images provide possible reasons for the increase in MCE to be the reduction in Ce_2Si_3 fraction and the increase in Ce_5Si_4 fraction. While XRD analyses and area fractions obtained from SEM images show relatively smaller changes in the phase fractions, optical microscopy images provide a larger field-of-view showing that the

change in phase fractions of Ce_2Si_3 and Ce_5Si_4 is indeed considerable to explain the improvement in MCE with the starting composition or annealing.

As an alternative to the 18-day furnace anneals, PNNL's annealing treatments with Joule-heating resulted in comparable improvements of the magnetocaloric properties (Figure 7). The improvements were mostly independent of the annealing time and temperature. Multiple anneals at 2, 4, 7, 24 hours at various temperatures ranging between 950-1050 °C, consistently resulted in about ΔS_{max} ~ 9 J/kgK. This value was about 20% lower than the 18-day furnace anneal ΔS_{max} = 10.9 J/kgK, but with a 150 °C lower annealing temperature.

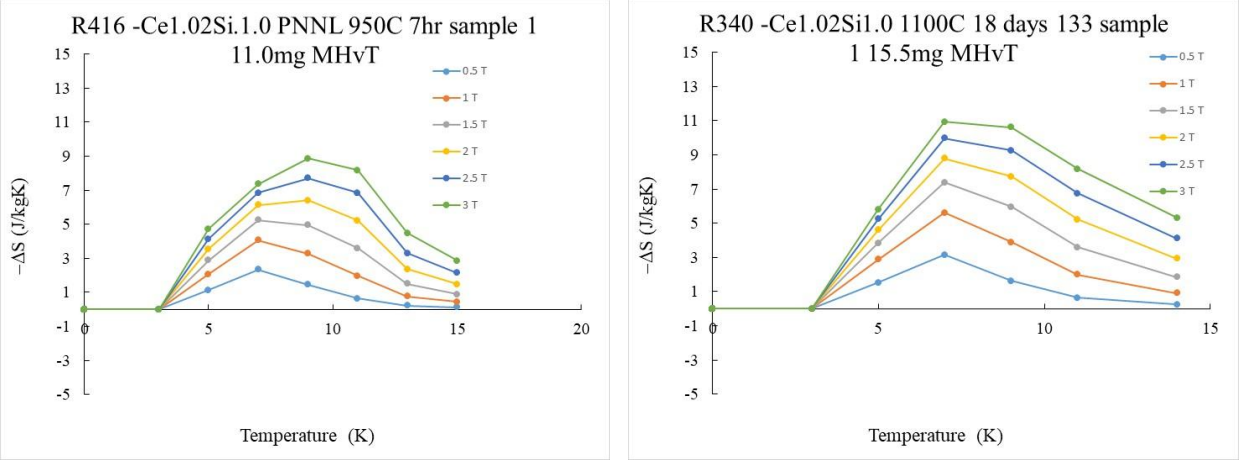

Figure 7. Magnetocaloric performance of PNNL Joule-heating annealed (left) and furnace annealed (right) of the off-stoichiometric $Ce_{1.02}Si$ alloy showing that the Joule-heated sample has similar magnetocaloric performance as the furnace annealed sample despite the lower temperature and shorter annealing time in the former.

With the promising results obtained in Joule-heating anneals, a similar annealing study was repeated with the furnace. Figure 8 summarizes the magnetocaloric properties obtained with the various furnace annealing treatments at 1100 °C and a lower temperature of 950 °C. Shorter anneals produce entropy change comparable to the typical 18 day (432 hr.) – 1100 °C annealing procedure. Annealing times of as lows as 7 hours resulted in ΔS_{max} = 10.3 J/kgK under 3 T magnetic field, slightly lower than the 18-day annealing value of 10.9 J/kgK. Further increase in annealing time to 24 and 72 hours at 1100 °C did not provide much improvement. For all the samples, SOPT temperature range was similar with ΔS_m peaking around 11 K. Magnetocaloric properties after annealing at 950 °C were also comparable to the longer and high temperature anneals, with ΔS_m ranging between 6.7-9.6 and peaking around 9.6 J/kgK at 9 K in the 24-hour annealed sample.

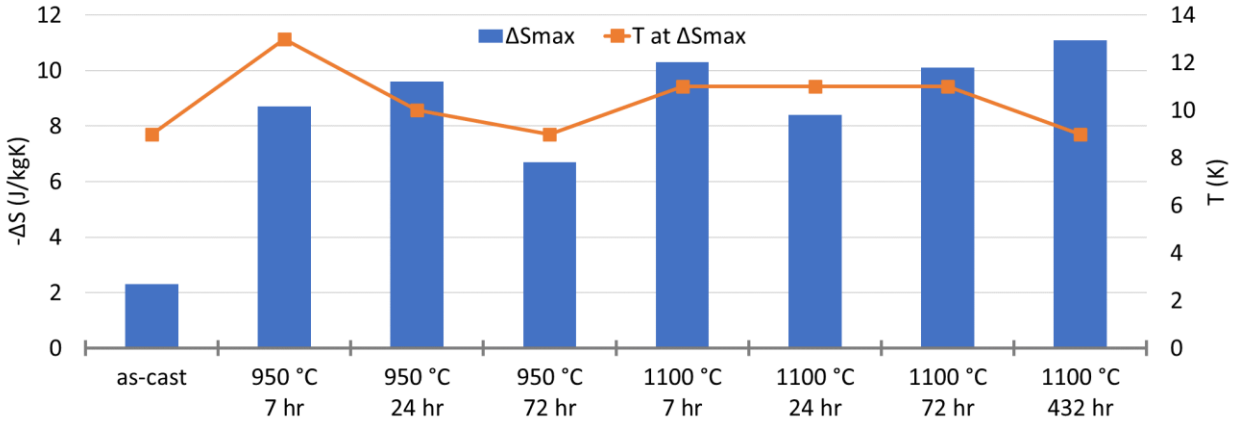

Figure 8. Magnetocaloric properties of $Ce_{1.02}Si$ in as-cast condition and after furnace annealing for various times and temperatures. The data shows that while annealing at 1100 °C for 432 hours (current practice) increases the magnetocaloric performance of as-cast material by up to ~5x, shorter annealing times and lower temperatures (within the ranges tested) are equally effective.

A simple calculation of the diffusion coefficient and distances explains why shorter anneals are equally effective in transforming the small fractions of Ce_2Si_3 phase into CeSi and Ce_5Si_4. As the diffusion coefficients for the Ce-Si system are not available, self-diffusion of bcc Ce was used for the calculations [29]. Table 2 shows the diffusion distances ($d = \sqrt{D.t}$) covered by the Ce atoms at the times and temperatures used in the annealing experiments. Self-diffusion of Ce is fast enough event at the lowest time and temperature to decompose the Ce_2Si_3 phase, which had an average size of ~6 µm calculated from the SEM images. In other words, Ce atoms can diffuse out of the Ce_2Si_3 phase to form the other phases. The main drawback of these calculations is the assumption of self-diffusion coefficient of pure Ce, which has a melting point of 798 °C. The diffusion of Ce will be much slower in the CeSi phase with a melting point of 1630 °C and complex orthorhombic crystal structure. Assuming the activation energy for diffusion scales linearly with the melting point, hypothetical Ce diffusion in the CeSi phase can still cover enough distance to decompose the Ce_2Si_3 phase within few hours at 950 °C. Another drawback of this simple calculation is the large volume change associated with Ce_5Si_4 transformation [24], which is not accounted for in the simple diffusion calculations. The large volume expansion can act as thermodynamic barrier preventing the Ce_2Si_3 to Ce_5Si_4 phase transformation.

Table 2. Calculated self-diffusion rates and distances of Ce for various temperature-time combinations.

	D_0 (m^2/s)	Q (eV)	D (m^2/s)	d (µm)
Ce in Ce 950 °C 7 hours	1.2×10^{-6}	0.932	1.7×10^{-10}	2092
Ce in Ce 1100 °C 7 hours	1.2×10^{-6}	0.932	4.6×10^{-10}	3391
Ce in Ce 950 °C 7 hours (Q x 2)	1.2×10^{-6}	1.864	2.5×10^{-14}	25

Both annealing methods resulted in similar improvements in ΔS_{max} and shortened the annealing time significantly. Contrary to our initial hypothesis at the beginning of the project, Joule-heating did not provide any additional benefits over furnace annealing and it did not accelerate the annealing kinetics. Therefore, an energy and cost analysis was performed on the furnace heating method only to understand the impacts of shorter anneals on the processing costs.

With the considerable decrease in annealing time from 432 hours to 7 hours, energy required for annealing per 1 kg of MCM decreases by 99%. Assuming a 0.075 $/kWh electricity price, energy costs decrease from $324 to only $5.25. A similar reduction is also possible in equipment costs as more annealing batches can be performed with a given furnace. Labor and consumable costs are fixed per batch and so is the capacity of the furnace, and therefore these costs do not change with annealing time. Despite the fixed labor and consumable costs, the reduction is energy and capital costs alone decrease the processing cost per kg of MCM by 87%. This reduction in the processing cost is higher than what was targeted at the start of the project, and it is expected to benefit the commercialization of MCM developed by GE&R.

Conclusions

Key Outcome: This project performed annealing and microstructural analysis on the CeSi alloy system, a magnetocaloric material developed by GE&R for use in magnetocaloric hydrogen liquification. A key outcome of this work was that it enabled GE&R to shorten their lengthy anneals from 18 days (432 hours) to just 7 hours, resulting in 99% lower energy consumption and 87% lower process costs, attributed primarily to reduced energy and equipment costs.

Experimental Capabilities Developed: PNNL integrated a Joule-heating system within a vacuum chamber that allowed oxidation-sensitive CeSi alloy to be annealed in a controlled atmosphere with less oxidation. GE&R acquired and installed a new vacuum arc-melter which allowed them to cast the CeSi in new shapes and with better chemical homogeneity.

Technical Progress and Scientific Understanding: GE&R showed a significant dependence of the magnetocaloric performance on the initial composition. Samples containing slightly higher cerium, to compensate for the evaporation losses during arc melting, had twice the entropy change compared to the stoichiometric CeSi. PNNL identified the critical microstructural phases in the CeSi system to obtain the highest magnetocaloric performance and showed that even small changes in phase fractions through annealing or composition control can lead to significant improvements in the magnetocaloric performance. Annealing of arc-melted and as-cast samples at 1100 °C for 18 days (432 hr.) decreased the Ce_2Si_3 phase fractions from 6% to 1%, which decomposed into Ce_5Si_4 and the main matrix phase of CeSi. Annealing did not change the grain size, morphology, or compositional homogeneity of the main CeSi phase. Despite the rather small changes in the phase fractions, annealing improved the magnetic entropy change from almost 0 to 11 J/kgK. Anneal durations as short as 7 hours produced similar improvements in the magnetocaloric performance, which was explained by the sufficient diffusion rates and distances of Ce atoms to decompose the detrimental Ce_2Si_3 phase. Joule-heating CeSi for a few hours resulted in similar improvements in its magnetocaloric performance compared to the conventional furnace heating. However, Joule-heating did not shorten the annealing time or accelerate phase transformation kinetics.

Subject Invention

N/A

References

1. Franco, V., et al., *The Magnetocaloric Effect and Magnetic Refrigeration Near Room Temperature: Materials and Models.* Annual Review of Materials Research, 2012. **42**(1): p. 305-342.

2. Ihnfeldt, R., et al., *Low-cost Magnetocaloric Materials Discovery*. 2019, DOE AMR presentation: https://www.hydrogen.energy.gov/.

3. Ihnfeldt, R., et al., *Magnetocaloric alloys useful for magnetic refrigeration applications*. 2022, GENERAL ENGINEERING & RESEARCH LLC

4. Ihnfeldt, R., et al., *Magnetocaloric alloys useful for magnetic refrigeration applications*. 2021.

5. *Magnetic Refrigeration Products*. 17 Aug 2023].

6. Wang, L.C., et al., *Low-temperature large magnetocaloric effect in the antiferromagnetic CeSi compound.* Journal of Alloys and Compounds, 2014. **587**: p. 10-13.

7. Ihnfeldt, R., et al., *Magnetic refrigeration systems for cryogenic applications*. 2022.

8. Belo, J.H., et al., *Phase control studies in Gd5Si2Ge2 giant magnetocaloric compound.* Journal of Alloys and Compounds, 2012. **529**: p. 89-95.

9. Yan, A., et al., *Effect of composition and cooling rate on the structure and magnetic entropy change in Gd5SixGe4−x.* Journal of Applied Physics, 2004. **95**(11): p. 7064-7066.

10. Pecharsky, A.O., K.A.G. Jr., and V.K. Pecharsky, *The giant magnetocaloric effect of optimally prepared Gd5Si2Ge2.* Journal of Applied Physics, 2003. **93**(8): p. 4722-4728.

11. Zhang, H., et al., *Phase relationships and crystallography of annealed alloys in the Ce5Si4–Ce5Ge4 pseudobinary system.* Journal of Alloys and Compounds, 2009. **487**(1): p. 98-102.

12. Hunagund, S.G., et al., *Investigating phase transition temperatures of size separated gadolinium silicide magnetic nanoparticles.* AIP Advances, 2018. **8**(5): p. 056428.

13. Liu, J., et al., *Influence of annealing on magnetic field-induced structural transformation and magnetocaloric effect in Ni–Mn–In–Co ribbons.* Acta Materialia, 2009. **57**(16): p. 4911-4920.

14. Hou, X., et al., *Formation mechanisms of NaZn13-type phase in giant magnetocaloric La–Fe–Si compounds during rapid solidification and annealing.* Journal of Alloys and Compounds, 2015. **646**: p. 503-511.

15. Potnis, G., et al., *Assessing two rapid quenching techniques for the production of La-Fe-Si magnetocaloric alloys in reduced annealing time.* Material Design & Processing Communications, 2019. **1**(6): p. e96.

16. Miao, X.-F., H. Sepehri-Amin, and K. Hono, *Structural origin of hysteresis for hexagonal (Mn,Fe)2(P,Si) magneto-caloric compound.* Scripta Materialia, 2017. **138**: p. 96-99.

17. Couillaud, S., et al., *The magnetocaloric properties of GdScSi and GdScGe.* Intermetallics, 2011. **19**(10): p. 1573-1578.

18. Morozkin, A.V., et al., *The Ce-Ni-Si system as a representative of the rare earth-Ni-Si family: Isothermal section and new rare-earth nickel silicides.* Journal of Solid State Chemistry, 2016. **243**: p. 290-303.

19. Zhang, H., et al., *Phase relationships, and structural, magnetic, and magnetocaloric properties in the Ce5Si4–Ce5Ge4 system.* Journal of Applied Physics, 2010. **107**(1): p. 013909.

20. Bulanova, M.V., et al., *Cerium–silicon system.* Journal of Alloys and Compounds, 2002. **345**(1): p. 110-115.

21. Gokhale, A.B., A. Munitz, and G.J. Abbaschian, *The Nd-Si (Neodymium-Silicon) system.* Bulletin of Alloy Phase Diagrams, 1989. **10**(3): p. 246-251.

22. Munitz, A., A.B. Gokhale, and G.J. Abbaschian, *The Ce-Si (Cerium-Silicon) system.* Bulletin of Alloy Phase Diagrams, 1989. **10**(1): p. 73-78.

23. Yashima, H., et al., *Spin-fluctuation effects in Ce-Si system.* Solid State Communications, 1982. **43**(8): p. 595-599.

24. Alanko, G.A., et al., *Mechanochemical synthesis and spark plasma sintering of the cerium silicides.* Journal of Alloys and Compounds, 2014. **616**: p. 306-311.

25. Vejpravová, J., et al., *Antiferromagnetic ordering in Ce5Si4.* Physica B: Condensed Matter, 2006. **378-380**: p. 784-785.

26. Snyman, J.L., et al., *Positive and negative magnetocaloric effects in CeSi.* Journal of Applied Physics, 2013. **113**(17): p. 17A903.

27. Shaheen, S.A. and J.S. Schilling, *Ferromagnetism of CeSix at ambient and high pressure.* Physical Review B, 1987. **35**(13): p. 6880-6887.

28. Smith, J.S., et al., *Electric, thermal, and magnetic properties of CeSix with $1.57<x\leqslant 2.0$.* Journal of Applied Physics, 2005. **97**(10): p. 10A905.

29. Dariel, M.P., D. Dayan, and A. Languille, *Self-Diffusion in fcc and bcc Cerium.* Physical Review B, 1971. **4**(12): p. 4348-4354.

Pacific Northwest National Laboratory

902 Battelle Boulevard
P.O. Box 999
Richland, WA 99354
1-888-375-PNNL (7665)

www.pnnl.gov